

 Open access • Journal Article • DOI:10.1002/ADHM.202001199

## **New Smart Antimicrobial Hydrogels, Nanomaterials, and Coatings: Earlier Action, More Specific, Better Dosing? — Source link**

Lorène Tallet, Lorène Tallet, Varvara Gribova, Varvara Gribova ...+6 more authors

**Institutions:** French Institute of Health and Medical Research, University of Strasbourg, Centre national de la recherche scientifique

**Published on:** 01 Jan 2021 - Advanced Healthcare Materials (John Wiley & Sons, Ltd)

**Topics:** Smart material

Related papers:

- [Advances in the Fabrication of Antimicrobial Hydrogels for Biomedical Applications](#)
- [Antimicrobial Nanomaterials Derived from Natural Products—A Review](#)
- [Biodegradable antimicrobial hydrogels and their use in biomedical purposes](#)
- [Antimicrobial Polymeric Structures Assembled on Surfaces.](#)
- [Recent trends in smart polymeric coatings in biomedicine and drug delivery applications](#)

Share this paper:    

View more about this paper here: <https://typeset.io/papers/new-smart-antimicrobial-hydrogels-nanomaterials-and-coatings-3200gsfwj3>

**New smart antimicrobial hydrogels, nanomaterials and coatings:  
earlier action, more specific, better dosing?**

*Lorène Tallet, Varvara Gribova, Lydie Ploux, Nihal Engin Vrana, Philippe Lavallo\**

\* Corresponding author

Dr. L. Tallet, Dr. V. Gribova, Dr. L. Ploux, Dr. P. Lavallo

Institut National de la Santé et de la Recherche Médicale, INSERM Unité 1121 Biomaterials  
and Bioengineering, 11 rue Humann, 67085 Strasbourg Cedex, France

Université de Strasbourg, Faculté de Chirurgie Dentaire, 67000 Strasbourg, France

Dr. N.E. Vrana, Dr. P. Lavallo

SPARTHA Medical, 14B Rue de la Canardiere, 67100 Strasbourg Cedex, France

E-mail: philippe.lavallo@inserm.fr

Keywords: smart surfaces, hydrogels, nanomaterials, coatings, antimicrobial

**Abstract**

To fight against antibiotic-resistant bacteria adhering and developing on medical devices, which is a growing problem worldwide, researchers are currently developing new “smart” materials and coatings. They consist in delivery of antimicrobial agents in an intelligent way, *i.e.* only when bacteria are present. This requires the use of new and sophisticated tools combining antimicrobial agents with lipids or polymers, synthetic and/or natural. In this review, we will describe three classes of innovative materials: hydrogels, nanomaterials and thin films. Moreover, smart antibacterial materials can be classified into two groups depending of the origin of the stimulus used: those that respond to a non-biological stimulus (light, temperature, electric and magnetic fields) and those that respond to a biological stimulus related to the presence of bacteria, such as changes in pH or bacterial enzyme secretion. The bacteria presence can induce a pH-change that constitutes a first potential biological trigger allowing the system to become active. A second biological trigger signal consists in enzymes produced by bacteria themselves. A complete panel of recent studies will be given focusing on the design of such innovative smart materials that are sensitive to biological triggers.

**1. Introduction**

In recent years, there is an increase in antibiotic-resistant bacteria<sup>[1]</sup> and a decline in development of new antibiotics.<sup>[2]</sup> The World Health Organization (WHO) has declared antibiotic resistance as one of the biggest threats to humanity. In the United States, the Center for Disease Control and Prevention (CDC) has estimated that two million patients per year suffer from infections that are due to drug-resistant bacteria.<sup>[3]</sup> If this trend continues, it is estimated to cause 10 million deaths worldwide in 2050 and a total cost of 100 trillion dollars.<sup>[4]</sup> Antibiotic resistance is anticipated to even escalate since antibiotics are excessively used worldwide not only in hospitals but also in food industry. In low- and middle-income countries,

the use of antibiotics increases with rising incomes, higher hospitalization rates and higher prevalence of hospital infections.<sup>[5]</sup> All these contribute to the selection pressure that maintains resistant strains, forcing to switch to increasingly expensive and broad-spectrum antibiotics.

Over the past 50 years, the use of biomaterials and medical devices such as catheters, joint implants and contact lenses has become more and more common. This increase is due to the aging of the world's population, as well as to advances in materials technology. The surface of such devices is conducive to bacterial adhesion and the resultant biofilm formation.<sup>[6]</sup> According to the US National Institutes of Health, biofilms account for over 80% of microbial infections in the body.<sup>[7]</sup> Once the biofilm is installed, treatment of the infection becomes more challenging. Indeed, the extracellular polymeric substance synthesized by bacteria in a biofilm provides a physical protection by restricting the transport of compounds, including biocidal agents, through the biofilm.<sup>[8]</sup> Furthermore, some bacteria living in the biofilm are in slow-growing or starved conditions with severely altered metabolic activity, which reduces their sensitivity to antibiotics.<sup>[9]</sup> To eradicate a biofilm, it is therefore necessary to increase the dose of antibiotic up to thousand times compared to that needed to eradicate planktonic bacteria.<sup>[10]</sup> Furthermore, the administration of antibiotic treatment is rarely localized, most of the patients being treated by intravenous injections or oral intake.<sup>[9b, 11]</sup> This causes selection pressure in the whole body and reduces the dose reaching the target site due to dilution and possible degradation of the drug molecules.<sup>[12]</sup> Thus, repeated or higher dose of drug is needed for an effective treatment of localized bacterial infections.

Special attention has been recently given to the design of coatings dedicated to the localized treatment of surface-related infections of medical devices. Several strategies have emerged, including prevention of adhesion of pioneer bacteria, killing of adhering bacteria by contact with the surface, and killing of all surrounding bacteria by drug release from the surface. Especially this latter strategy is expected to result in an effective and safe infection treatment

due to the administration of high dose of antibiotics locally around the infection site. Most of the antibacterial coatings and materials seeking local administration of antibiotics have a similar release profile that can be split into two phases: a phase with rapid release of antibiotics (sometimes referred to as burst release) and a second phase with slow release, often over a few days.<sup>[11, 13]</sup> Their antibacterial efficacy has been demonstrated many times. However, antibacterial molecules are released both in presence and in absence of the infection. This results in the fast depletion of the drug supply and may facilitate the development of resistant strains of bacteria, cytotoxicity and damage of tissues. Therefore, smart antibacterial systems, *i.e.* systems targeting bacterial infections and responsive to the bacterial microenvironment have been increasingly studied in recent years (**Figure 1**). Their ability to adjust the release of antibiotics according to the bacterial contamination allows for better efficacy of the antibacterial treatment by increasing the local drug concentration at the infected site. This strategy makes it possible to also limit the accumulation of drug in healthy host tissues, minimizing the risks of toxicity and bacterial resistance as well as collateral damages to the commensal microflora.<sup>[14]</sup> Smart antibacterial coatings can be classified into two groups, responding to either non-biological or biological stimulus. In the first class of coatings the release of antibacterial molecules is induced by an external event such as light,<sup>[15]</sup> temperature,<sup>[16]</sup> electric or magnetic fields<sup>[17]</sup>. For example, Zhang and co-workers<sup>[18]</sup> developed a photon-controlled antibacterial platform for skin infections that efficiently killed resistant bacteria. They encapsulated black phosphorous quantum dots (BPQDs) inside thermal-sensitive liposomes. Drug encapsulated inside liposomes then released in a spatial-, temporal- and dose-controlled fashion due to disruption of the liposomes under near-infrared light stimulation of BPQDs. The second class of coatings includes stimuli directly related to the presence of bacteria, thus it can be considered as an “internal” stimulus. To make this possible, the researchers relied on the differences that exist between a healthy and an infected environment. The microenvironment of a bacterial

infection site especially differs from healthy tissues by the abundance of extracellular enzymes and by the pH. Indeed, through their life cycle, bacteria produce and release many enzymes such as hyaluronidases (HAase), chymotrypsin (CMS), lipases, metalloproteinases, and other extracellular proteins.<sup>[19]</sup> For example, *Staphylococcus aureus*, gram-positive bacteria usual on skin and mucosa in a third of the population, are versatile human pathogens that secrete four major extracellular proteases *i.e.* a metalloproteinase, a serine glutamyl endopeptidase and two related cysteine proteinases,<sup>[19c]</sup> as well as hyaluronidase in a smaller amount.<sup>[20]</sup> The presence of these enzymes can be exploited as a stimulus to cleave components of an adequate coating thus triggering the release of molecules including antimicrobial agents. This strategy should allow the build-up of enzyme-triggered antibacterial systems specific to a particular genus or species. The second parameter that is different between infected site and normal tissues is pH. When a device is colonized by bacteria, the metabolites they produce accumulate in the environment surrounding the device leading to a pH change. Especially in biofilms, anaerobic bacteria can grow in aerobic environments, which favors fermentation and lead to acidification.<sup>[21]</sup> On the other hand, when a wound is infected, the pH of the skin (normally between 5.4-5.6) tends to increase because the underlying tissue with pH of 7.4 becomes exposed.<sup>[22]</sup> This promotes proliferation of commensal skin species, which leads to alkalization of pH by production of ammonia by bacteria.<sup>[23]</sup> Thus, pH does not vary in the same way from one tissue to another. The intended application of the coating must therefore be considered when using pH as a triggering stimulus for antibacterial activity.

Among both classes of stimuli, the biological-based one that consists in using the presence of bacteria and their metabolites is the most promising in term of simplicity as it is a “passive” system that will not require any external triggering. An external stimulus means that first the infection should be detected (through monitoring physiological parameters for example) and only then the external trigger will be activated. Thus, this time delay in the response can be

important and can lead to infections that can no longer be cured. Systems with non-biological-related stimulus require either systematic stimulus or a two-step procedure with as first the detection of the infection (through monitoring physiological parameters for example) and secondly activation of the trigger. The first detection step is difficult to achieve in some cases, especially for implanted devices. On the opposite, biological responding systems can be triggered as soon as few bacteria are close and before detecting a widespread infection. They can be therefore expected to have higher sensitivity.

Herein, we will focus on these attractive bacterial-induced triggering systems and summarize the recent research progresses in this sphere. We will especially deal with three materials, hydrogels, nanomaterials and thin films designed to be responsive to the pH changes and enzyme secretions.

## **2. Antimicrobial smart hydrogels**

Hydrogels are three-dimensional networks of hydrophilic cross-linked polymers that can respond to fluctuations of the environmental stimuli. They possess a degree of flexibility very similar to natural tissues due to their large water content. Hydrogels are already used in a large number of biomedical applications, such as tissue engineering, wound dressings, contact lenses etc. By changing the type and composition of the polymer precursor and the environment (pH, temperature), the degree of crosslinking and the mechanical properties of the hydrogels can be tuned according to the intended application. Besides, hydrogels are a versatile tool that allows, in particular, loading of drugs and their release in a controlled manner. This is achieved by adjusting the mechanical and chemical properties of the network. Usually hydrogels have relatively fast release profiles due to the high degree of hydration. Triggering this release can be achieved by the use of pH or enzyme stimuli.

## 2.1. pH-responsive hydrogels

Many antibacterial hydrogels were designed to respond to pH variations. Albright and co-workers<sup>[24]</sup> developed a layer-by-layer (LbL) hydrogel coating of poly(methacrylic acid) (PMAA) and poly(vinyl caprolactam) (PVCL) loaded with gentamicin. Alternating layers of PVCL and PMAA were constructed *via* spin-assisted deposition and were cross-linked *via* ethylenediamine. As shown in **Figure 2A**, PVCL was removed from the LbL after crosslinking by slowly adjusting the pH of the solution to 8 to form PMAA hydrogel-like coating. Carboxylic groups of PMAA can act as negative charges that bind positively charged antibiotics. Gentamicin was loaded in the hydrogel at pH 7.5, and its release in solution was tested at various pH. When the hydrogel was immersed in a pH 7.5 solution, 70% of the drug was released in the medium. The percentage of released antibiotics increased with decreasing pH of the solution (**Figure 2C**). This phenomenon is related to the degree of ionization of the PMAA, and is consistent with the swelling behavior shown in **Figure 2B**. However, some passive release already occurred at pH 7.5 considered as the pH value in the absence of infection. Therefore, complete suppression of the release at physiological pH cannot be achieved and a steady dose of antibiotics is supplied. In another work, PMAA derivative has been used to encapsulate silver nanoparticles in hydrogel matrices.<sup>[25]</sup> Poly(methyl methacrylate-co-methacrylic acid)/silver nanoparticles (P(MMA-co-MAA)/AgNPs) copolymer networks were made with various ratios of the components in order to modulate porosity and swelling behavior of the hydrogel network depending on the pH of the medium. The resulting modulation of pores size allowed the control of diffusion of Ag<sup>+</sup> ions.

Zhou *et al.*<sup>[26]</sup> have also created a LbL hydrogel coating that responds to pH variation. They have built a bi-functional coating that can both detect and inhibit bacterial infection by modification of the surrounding pH. This hydrogel was specifically designed for urinary catheters and is composed of 3 different layers (**Figure 3**): an inner layer of hydrogel PAA



(poly (acrylic acid)), a middle layer of chitosan (CH) and a pH-responsive layer of EudragitS100, a commercial co-polymer of methyl methacrylate and methacrylic acid. Polydiacetylene (PDA) vesicles encapsulating ciprofloxacin (CIP) were integrated into the PAA and CH hydrogel layers, which were alternately deposited through electrostatic interactions by adjusting the pH values of the solution. Urease-producing species like *Proteus mirabilis* are able to hydrolyse urea, leading to elevation of the urinary pH. The PDA vesicle system showed a chromatic color transition visible by naked eyes from blue in acidic media (pH < 7), to purple and red in alkaline media (pH 7–8.8 and pH > 8.8, respectively) at physiological temperature. In addition to being able to detect the presence of an infection in the urine, this coating can also limit the bacterial infection. Indeed, at pH < 7, no CIP was released since PDA vesicles were not released from the coated polymers. However, release rate increased for increasing pH values due to gradual diffusion of the “trigger layer” of EudragitS100, causing gradual release of PDA vesicles into the external medium. This coating allowed a significant reduction of the number of viable *P. mirabilis* (initially  $7.10^5$  CFU.mL<sup>-1</sup>) after overnight incubation. Unlike *P. mirabilis*, *E. coli* is a urease-negative species that thus does not generate alkalinisation of the medium and subsequent degradation of the EudragitS100 layer. It was therefore used as a control species. As expected, it was not affected by the coating and the number of viable cells increased over time. Thus, this smart coating has been shown not only to specifically recognize the presence of urease-producing pathogenic bacteria in urine solution and to send a corresponding colorimetric signal, but also to inhibit their proliferation. Another way to create a pH-sensitive hydrogel is to incorporate Schiff bases. [17b,27] Schiff bases are compounds with a C = N double bond, which is unstable at acidic pH. By integrating Schiff base into a hydrogel, it is thus possible to induce gel degradation by varying the pH. For instance, the Schiff base which is formed between—CHO of oxidized dextran and—NH<sub>2</sub> of chitosan allows the formation of such hydrogel. [17b] The hydrogel can be loaded with an antibacterial

agent such as amoxicillin by mixing it with the two other components before gelation. In this study, the antibacterial agent is thus simply encapsulated in the gel matrix. About 55% of the drug was released after 36 h of immersion in a PBS solution at pH 7.4, while, in a PBS solution at pH 5.5, 99% of the drug was released over the whole period of 36 h. With this formulation, there is nevertheless a non-specific *i.e.* passive release due to the simple diffusion of the antibiotic into the supernatant.

To avoid the passive diffusion of the antibacterial agent, aminoglycoside antibiotics can be preferred. These antibacterial molecules have from three to six primary amine groups that can therefore serve as linkers via a Schiff base formation to create hydrogels when mixing them with oxidized polysaccharides. Indeed, polysaccharides are good candidates for the manufacturing of these hydrogels since they are natural polymers which provides for most of them an excellent biocompatibility. They also mostly have high aqueous solubility and biodegradability properties. Hu *et al.*<sup>[27a]</sup> have screened a large number of aminoglycoside/polysaccharide combinations (**Figure 4a**). The authors particularly studied amikacin/dextran aldehyde (Dex-CHO) hydrogel for its suitable gelation time (~1 min) and the broad-spectrum antibacterial activity of amikacin in clinical applications. The hydrogel weight decreased by 36% and 45% when it was immersed in a buffer solution at pH 6.0 and pH 5.0 for 24 h, respectively (**Figure 4c**). In comparison, when the gel was kept in a pH 7.4 buffer solution, no weight loss was observed. As shown in **Figure 4d**, these hydrogels display, in addition, a self-healing property: they are able to reform once environmental conditions have returned to normal *i.e.* physiological pH. The erosion-based drug release behavior of this hydrogel avoids burst release of drugs and allows it to synchronize with gel degradation. Several other studies have been described with pH responsive hydrogels built with aminoglycoside as antibiotics<sup>[28]</sup> Dex-CHO was used in another study in complexation with cationic dendrimers (amine-terminated generation 5 (G5) polyamido-amine (PAMAM)) and AgNPs.<sup>[27b]</sup> In an acidic

environment, the release ratio of AgNPs and G5 was two times higher than in a neutral environment after 24 h. Moreover, the combination of cationic dendrimers and AgNPs showed a synergistic effect in the treatment of bacterial infections.

Dynamic covalent gels consisting of tannic acid and boronic acids show also acid- base-reduction- and oxidant- sensitive properties. Tannic acid is known to destabilize the bacteria membrane and consequently tannic acid/borate gels show antibacterial activity towards *E. coli*.<sup>[29]</sup>

Another way to insert a Schiff base in a hydrogel is to use polyethylene glycol (PEG). Bu and co-workers<sup>[27c]</sup> created hydrogels with 3 different PEGs: 4-arm-PEG-NH<sub>2</sub>, 4-arm-PEG-NHS, and 4-arm-PEG-CHO loaded with vancomycin, a first-generation glycopeptide antibiotic (**Figure 5**). Three hydrogel formulations were made by tuning the ratios between the different PEGs. The number of Schiff bases present in the hydrogel varied according to its composition, and the gel called “Gel3” was built with a higher number of Schiff bases compared to the gel called “Gel2”. The gel “Gel1” did not contain any Schiff base. Only 21% and 28% of vancomycin was released from the Gel 2 and the Gel 3, respectively, at pH 7.4, while 78% and 93%, respectively, were released at pH 5. These results suggest that the increasing number of Schiff bases makes the hydrogel more pH-sensitive and is responsible for an increase in vancomycin release. These results have been confirmed *in vitro* antibacterial activity studies, which revealed a better antibacterial activity of Gel 3 (the one containing the most Schiff bases) compared to the others. *In vivo* tests were performed on a rabbit infection model with Gel 2, which was selected for having suitable combination of mechanical strength, adhesion and release rate. *In vivo*, haemostatic and antimicrobial experiments shown that hydrogels can inhibit the growth of *S. aureus* bacteria and can stopped the blood loss. In addition to the antibacterial activity of vancomycin, PEG hydrogels reduce the initial attachment of bacteria.<sup>[30]</sup>

The previously described hydrogels responded to a decrease in pH. However, in case of topical applications, the acidic environment of the wound becomes basic in the presence of infection. Hydrogels are well-suitable for wound applications because they help to maintain a wet environment that is favourable to reduce pain, promote cell mobility, and maintain hydration and tissue structure.<sup>[31]</sup> A hybrid hydrogel with keratin and zinc oxide nanoplates (nZnO) was developed by Villanueva and co-workers for such purpose.<sup>[32]</sup> Keratin hydrogels demonstrated a pH-dependent swelling profile: they swelled more when pH increased. This characteristic allowed the pore size to increase in presence of bacteria and therefore with an increase in pH. This is accompanied by an increase in the water content that shifts the dissolution equilibrium of the nanoparticles by promoting the release of  $Zn^{2+}$ , the biocidal agent in this study. Zhu *et al.*<sup>[33]</sup> also developed a hydrogel for an antibacterial wound dressing application. The hydrogel, composed of peptide-based bis-acrylate and acrylic acid (AAc), exhibited a pH-dependent swelling behaviour (**Figure 6**). Four different gels were produced, with the ratio of peptide-based bis-acrylate to AAc increasing from gel 1 to gel 4. The pore sizes decreased with the increase in peptide-based bis-acrylate contents, the cross-linker. The swelling ratio for these hydrogels increased when the solution became alkaline (**Figure 6**). Indeed, hydrogen-bonding interactions between the free carboxylic acid groups of the hydrogel network were stronger in an acid environment, which led to a lower swelling ratio. In alkaline media, where hydrogen bonds would be broken and electrostatic repulsions could repel chain segments, the hydrogel was expected to have higher swelling ratio and thus to favour the release of the drug. These peptide-based bis-acrylate/AAc hydrogels loaded with triclosan as a drug were applied on bacteria and provided a fast drug release, thus achieving killing of the bacteria in a short period of time.

## 2.2. Enzyme-triggered hydrogels

Another way to create hydrogels responding to a bacterial stimulus is to use proteases and virulence factors produced during an infection. Zhou *et al.* [34] designed a hydrogel able to respond to toxins or enzymes secreted by pathogenic bacteria such as *S. aureus* or *P. aeruginosa*. They developed vesicle of phospholipid bilayer membranes with encapsulated antibiotics or fluorescent dye to kill bacteria in addition to giving fluorometric indication when infection occurs. Vesicles were embedded into biocompatible gelatin methacryloyl (GelMA) for long term use in wound dressing. Two types of vesicles were loaded in the hydrogel: vesicles containing an antibiotic agent (gentamicin sulfate (GS) or silver nitrate) and vesicles containing carboxyfluorescein, the fluorescent dye. Carboxyfluorescein encapsulated at high concentration is non-fluorescent, but becomes fluorescent when the dye is diluted as a result of the degradation of the vesicle membrane. To test the ability of bacteria to degrade the phospholipid membrane, two pathogenic strains (*S. aureus* and *P. aeruginosa*) and one non-pathogenic strain (*E. coli*) were used. Hydrogels were deposited onto wound dressings and incubated for 4 h at 37 °C with bacterial suspensions before counting of the viable, adherent bacteria. Samples showed a significant reduction in the number of viable cells for the two pathogenic bacteria and no effect was shown for the non-pathogenic strain of *E. coli*. These results correlated with the fluorescence intensity, which showed that the non-pathogenic bacteria were unable to disrupt vesicle membranes. Only toxins and enzymatic factors from *S. aureus* and *P. aeruginosa* were able to damage the phospholipid vesicles. An *in vivo* experiment was performed by using a murine skin wound-healing model, which demonstrated that the dressings applied on wound sites infected with pathogenic bacteria provided fluorescence under low UV light, whereas no fluorescence was detected with the non-pathogenic bacteria (**Figure 7**). Both *in vitro* and *in vivo* experiments showed the ability of the wound dressing to selectively inhibit pathogenic bacteria without responding to commensal ones. This theranostic system is very promising

because it can indicate the presence of infection and respond to pathogenic bacteria simultaneously and, besides promoting wound healing due to the hydrogel properties.

### **3. Antimicrobial smart nanomaterials**

There are many ways to use nanomaterials to make drug delivery systems. They can be used in solution, immobilized on a surface, integrated in a hydrogel or in a coating. In this part, we will especially address the use of nanomaterials in solution.

#### **3.1. pH-responsive nanomaterials**

Nanomaterials are increasingly used for drug delivery in cancer tumours. Like infectious environment, cancerous tissues have a lower extracellular pH, compared to healthy tissues. It is therefore possible to combine delivery of anticancer and antibacterial drugs. Zeynabad *et al.* [35] proposed a multifunctional drug delivery system based on cationic silica-based polymer-clay nanocomposite for such combined therapy. The nanocomposite (NC) was loaded with two anticancer and one antibacterial agent, ciprofloxacin (CIP). The drug release behavior was pH dependent: About 5-10% of the three drugs were released under physiological conditions (pH 7.4) after 600 h, whereas (pH 4), the release reached 100% at lower pH. This was attributed to the electrostatic interactions between drugs and nanoparticles that prevent the release at pH 7.4, while at lower pH, the degree of ionization changes and the nanoparticles can thus release the drugs.

Montari and co-workers [36] have developed nanoparticles made of hyaluronic acid (HA) and tannic acid (TA). The presence of HA allows these organic particles to target bacteria that colonize cells presenting HA membrane receptors such as macrophages. HA modified with 3-aminophenyl boronic acid groups (HA-APBA) can react with TA by forming boronate ester bond. These NPs swell and dissolve in acidic conditions while they are stable under neutral conditions. Catechol-boronate complexation maintains TA in the reduced (catechol) form,

allowing the release of an active form of TA under acidic conditions. Sims et al. [37] also designed pH-responsive polymer nanoparticle carriers loaded with farnesol, a hydrophobic antibacterial drug. Their goal was to develop nanoparticles to fight oral infection diseases. The NPs, built with p(DMAEMA)-b-p(DMAEMA-co-BMA-co-PAA) and combined with a saturated farnesol solution, revealed a release half-time ( $t_{1/2}$ ) of 22.9 hours at pH 4.5 and 36.6 hours at pH 7.2. In the presence of bacteria, the environmental acidification also accelerated the drug release necessary to kill bacteria: the pH-responsive release led to a difference in CFU.mL<sup>-1</sup> reduction of approximately 2 log between pH 7 and pH 5 against 16-hours *S. mutans* biofilms. The anti-biofilm activity was also tested with another drug, thonzonium bromide (TB). TB-loaded NPs resulted in the reduction of bacterial viability by about 6 log CFU.mL<sup>-1</sup>.

As for hydrogels, Schiff bases are interesting for creating pH-sensitive systems. Dynamically cross-linked polymer nanocomposites created by Zhu et al. integrate Schiff bases for taking advantages of the acidic microenvironments within biofilms.<sup>[38]</sup> A poly(oxanorborneneimide) scaffold bearing guanidine, amino, and tetraethylene glycol monomethyl ether groups (PONI-GAT), an adamantyl-core tetrakisaldehyde (ATA) crosslinker, and carvacrol oil are used to design an antimicrobial nanocomposite (**Figure 8a**). In the presence of ATA, PONI-GAT amines crosslink with ATA aldehydes, generating NCs. The NCs appear spherical through transmission electron microscope imaging (**Figure 8b**) and have average size of 220 nm measured by dynamic light scattering (**Figure 8c**). After 3 h in contact with a biofilm, the NCs led to the reduction of cell viability by more than 90% within the biofilm, thus showing that the nanocomposites were able to penetrate the biofilm and to kill almost all the bacteria within.

Finally, NCs can be further used in combination with a coating. The most common way is to produce NCs first before immobilizing them onto the coating surface. In that respect, poly(vinyl alcohol) (PVA)/poly(lactide-glycolide acid) (PLGA) NPs with encapsulated vancomycin (Van) were grafted onto the surface of titanium for creating a pH-sensitive drug delivery coating.<sup>[39]</sup>

The addition of aminopropyltriethoxysilane (APTES) on the titanium surface allowed the grafting of the PVA/PLGA NPs through the formation of amide bonds. Ester bonds between PVA and PLGA being easily cleaved under acidic condition, the release of Van was triggered under bacterial infection conditions.

### 3.2. Enzyme-triggered nanomaterials

To create nanocomposite-based smart systems, nanoparticles are often combined with liposomes. Since the membrane of liposomes is similar to that of the cell membrane, the toxins secreted by bacteria can easily interact with them. Pornpattananankul and co-workers<sup>[40]</sup> used chitosan-modified gold nanoparticles (AuCH) to stabilize liposome with encapsulated Van, thus avoiding their fusion and subsequent unexpected antibiotic leakage. In this study, the triggering signal is given by a toxin secreted by *S. aureus*, alpha hemolysin, also named  $\alpha$ -toxin. This protein is able to form pores in the outer membranes of susceptible cells and thus to generate cell lysis. The mechanism is the same for the liposome: In the presence of bacteria and therefore of the toxin, pores are formed through the lipid bilayer membrane of the liposome, which results in the release of the antibiotic causing the death of the surrounding bacteria.

Some bacteria, for example *S. aureus*, can invade host cells, e.g. macrophages and osteoblasts, to escape the immune system.<sup>[41]</sup> Most antibacterial agents have a limited ability to act on such intracellular bacteria, which makes them difficult to be eliminated. Nanomaterials are good candidates for targeting intracellular bacteria. Yang *et al.*<sup>[42]</sup> designed toxin-sensitive intracellular antibiotic delivery nanocomposites. These NCs are made of a mesoporous silica core loaded with GS, a lipid bilayers surface shell and a cationic human antimicrobial peptide fragment, ubiquicidin (UBI<sub>29-41</sub>), anchored onto the shell (**Figure 9**). The liposome layer was expected to help avoiding non-specific release of antibiotics and to allow NCs to target bacteria in infected tissues. In the presence of phosphatase, lipase and phospholipase secreted by



bacteria, the outer layer of the liposomes is degraded, leading to exposure of GS and elimination of bacteria. The authors finally showed the interest of combining bacteria-triggered release of antibiotics, with the control of the delivery location i.e. into the cytosol, by targeting cells thanks to UBI<sub>29-41</sub>.

Xiong and co-workers<sup>[43]</sup> also developed a nanogel capable of delivering drugs into infected macrophages. They have created a triple-layered nanogel (TLN, average diameter of about 420 nm) made of a bacterial lipase-sensitive poly( $\epsilon$ -caprolactone) (PCL) interlayer between the cross-linked polyphosphoester core and the shell of poly(ethylene glycol). Nanogels were loaded with Van (TLN-V). In the absence of lipase, the cumulative release of total encapsulated drug over 48 h of incubation in Tris-HCl buffer was very low (10%). In presence of *P. aeruginosa*'s lipase, a rapid release of Van was observed due to the rapid degradation of the PCL interlayer, and the release rate was dependent on the concentration of lipase. With 0.5 mg.mL<sup>-1</sup> of lipase, the cumulative release of Van reached 40% after 48 h, whereas with 1 mg.mL<sup>-1</sup> of lipase, the cumulative release achieved 70%. Ability of bacteria to trigger the system was tested by incubating nanogels with a bacterial suspension of *S. aureus* MW2 (high lipase secretion) or *E. coli* strains TOP10 and BL21 (low lipase secretion). Without bacteria, only 1% of total encapsulated Van was released after 1 h of incubation. With bacteria, a significant difference was observed between *S. aureus* MW2 and *E. coli* TOP10 and BL21 with respectively about 80%, 11% and 8% of Van released after 1 h of incubation. Researchers also examined whether the nanogel system is able to deliver drug in bacterial-infected cells. Cell penetration of nanogels was investigated by encapsulating a not membrane-permeable fluorescent dye, propidium iodide (PI), instead of Van, and following the nanogel behaviour in a culture of macrophages (mouse cell line). Cellular uptakes and releases of PI from the nanogels into cells infected or not with a green fluorescent protein (GFP)-expressing *S. aureus* strain were observed by using confocal laser scanning microscopy. PI and GFP-expressing *S.*

*aureus* were shown to be co-localized. In addition, PI was found in the nucleus, confirming the degradation of the nanogels by the bacteria. Finally, the ability of nanogels to kill intracellular bacteria was examined. As shown in **Figure 10**, nanogels with encapsulated Van had a better antibacterial activity against intracellular bacteria compared to Van in solution. Nanogels thus appear to be very promising to exhibit efficient antibacterial activity both against extracellular and intracellular bacteria while only releasing a very low dose of Van in absence of lipase or lipase-secreting bacteria.

In dentistry, recurrent or secondary caries, caused by acid-releasing cariogenic bacteria at the restoration-tooth interface, is a major cause of restoration failure and replacement.<sup>[44]</sup> Addition of antimicrobial agents into the restorative materials may affect the integrity of the materials, but also has limited release period. In this context, therefore, smart antimicrobial systems based on biological stimuli are particularly attracting. Stewart and co-workers<sup>[45]</sup> developed mesoporous silica nanocomposites loaded with antimicrobial amphiphilic drug, octenidine dihydrochloride (OCT), for such applications. The loaded NCs were incorporated in a dental resin adhesive that is usually placed between the composite and remaining tooth. The drug incorporated into NCs is expected to be release after stimulation by bacterial enzymes and for a long period of time. Commercial dental resins are readily degraded by enzymes present in human saliva, both of host and bacterial origin. The researchers used these enzymes to activate the antibacterial system *via* breakdown of the resin polymer matrix. They showed that the total release of drug increased by about 1.5 times in a simulated human salivary esterase, compared to PBS. These results indicate that the breakdown of polymer matrix and the release of loaded drug are related. The antibacterial activity of the modified resin was determined by incubating it with *S. mutans* and measuring subsequent cell viability. Thus, NCs showed a significant activity of reduction of the cell viability (4.4 log), suggesting that the local concentration of

OCT due to release triggered by bacterial esterase is sufficient to inhibit *S. mutans* growth. This system presents an advantage of confining the drug release, thus limiting systemic exposure.

#### 4. Smart responsive multilayer thin films

##### 4.1. pH-responsive films

Multilayer films are widely used for manufacturing of antibacterial coatings. Especially layer-by-layer (LbL) assembly of polyelectrolytes can be used as a multifunctional platform allowing the combination of both antibacterial and stimuli-responsive properties. CH is widely used to create pH-sensitive LbL-based coatings. It is a linear cationic polysaccharide with inherent antimicrobial properties, whose protonation of amino groups generates positively-charged polymer chains. This results in films swelling specifically in an acidic aqueous environment (below  $pK_a \sim 6.3$ ). CH is therefore particularly appropriate as a component of pH-sensitive system. Nalam *et al.* [46] studied the nanomechanical properties of pH responsive bilayer films composed of CH and poly(acrylic acid) (PAA), another pH-sensitive polymer. The first layer of PAA was grafted onto the surface to create a brush, which can be cross-linked with CH chains, forming the second layer. The swelling ratio ( $S_r$ ) of this coating is higher at pH 4.0 ( $S_r \sim 260$ ) than at pH 7.4 ( $S_r \sim 102$ ). When the antibiotic tobramycin (TOB) was loaded into the film, the film was observed to collapse and its thickness to decrease at both pH. In fact, the competitive interactions between TOB and water molecules with PAA brushes modify the solvation state of the PAA brushes in the CH/PAA coating at both pHs. Nevertheless, in an acidic environment, the PAA layer protonates and collapses and the CH layer swells, allowing the TOB molecules to be released and to diffuse into the surrounding medium (**Figure 11**). Antibacterial activity of the bilayer film tested against *S. aureus*, [47] showed that CH/PAATOBS could only prevent colonization by low amount of bacteria (about  $10^4$  CFU.mL<sup>-1</sup>). However,

the authors noted that the amount of loaded antibiotics may be adjusted by varying the thickness of PAA layer and thus the cross-linking of CH with PAA at the bilayer interface.

Wang and co-workers<sup>[48]</sup> have constructed LbL films with micelles, also based on CH and PAA. Micelles were composed of CH and methoxy poly(ethylene glycol)-poly( $\epsilon$ -caprolactone) (MPEG-PCL-CH), and could be loaded with a hydrophobic drug such as triclosan (TCA). As shown in **Figure 12**, free micelles released 92% of TCA after only 8 h. Their incorporation into a multilayer film by alternating micelles and PAA layers enables adjustment of the release rate. Thus, in this system, only 30% of TCA was released after 8h at pH 7.4. At pH 5.5, the rate of TCA release was enhanced because of the pH-responsive properties of CH and PAA. In order to verify whether the bacteria were capable of inducing antibiotic release by acidification of the medium, TCA release profile of the multilayer films was followed in the presence of bacteria. The level of TCA release increased when bacterial concentration was higher. Local acidification of the medium by bacteria thus allowed the release of TCA, which exerted its antibacterial power. In another study, Chen *et al.*<sup>[49]</sup> used MPEG-PCL-CH with montmorillonite (MMT) to construct multilayer films. They chose MMT for its excellent drug retention properties in a multilayer film. As for the precedent study,<sup>[48]</sup> this hybrid film displayed a pH-responsive release of TCA.

In order to increase density of antimicrobial material on the coating surface, Sutrisno and co-workers<sup>[50]</sup> used CH nanofibers (NF) on which they deposited a multilayer film. Nanofibers composed of CH and PCL were deposited through an electrospinning method on titanium substrates previously coated with polydopamine (PDop). Then, five bilayers of tannic acid/gentamicin sulfate (TA/GS) were added using a dipping method. The drug release rate of the so-formed Ti-PDop/NF/LbL was affected by pH. At low pH, TA was increasingly protonated, resulting in electrostatic repulsion, which thus achieved the release of GS from the substrates. Ti-PDop/NF/LbL showed a higher release of GS compared to Ti/LbL substrates.

This trend was explained by the larger surface area of nanofibers compared to native Ti substrate, which resulted in the deposition of a larger amount of GS per area unit. This high concentration of GS on the Ti-PDop/NF/LbL surface improved the antibacterial activity.

Sukhishvili *et al.*<sup>[51]</sup> also described the use of LbL to build pH-sensitive films, using montmorillonite (MMT) clay platelets and polyacrylic acid. They demonstrated that in physiological conditions, gentamycin remains sequestered for months in the film, but as soon as an acidification occurs due to the presence of bacteria, gentamycin is released. The same group also reported tannic acid/cationic antibiotic (like gentamicin, tobramycin and polymyxin B) to build LbL films. An antimicrobial “self-defense” mechanism was described as the film release antibiotics when pH is decreased by bacteria.<sup>[52]</sup>

Introduction of a three-dimensional (3D) structure on the material surface is another strategy for increasing the surface area covered by a bioactive multilayer film. Yan *et al.*<sup>[53]</sup> added a 3D porous structure onto polyetheretherketone (PEEK) surface. After sulfonation treatment, a layer of PDop was deposited on the surface, and AgNPs were added above. Then, three layers of silk fibroin were spun onto the surface, which was then immersed into a solution of GS. Finally, another three layers of silk were deposited. The combination of AgNPs and GS exhibited synergistic bacteria-killing effect on both Gram-positive (*S. aureus*) and Gram-negative (*E. coli*) bacteria (**Figure 13**), showing higher bactericidal effect than that of untreated PEEK. When pH decreases because of infection, protonation degree of silk fibroin and the number of positive charges increases, resulting in the release of positively charged Ag<sup>+</sup> and GS to maintain electroneutrality. Silk fibroin plays a key role in this coating: it confers a pH-dependent release of biocidal agents (Ag<sup>+</sup> and GS), acts as a barrier to prevent potentially adherent mammalian cells from being in direct contact with the underlying AgNPs and increases the contact angle, which is better for mammalian cell adhesion. Finally, this 3D porous coating has a dual function: bacteria-triggered bactericidal effect and improvement of osteogenic capacities.

The problem with most coatings is that after a while, the corpses of bacteria accumulate on the surface, preventing their antibacterial activity. In order to avoid this, Yan and co-workers<sup>[54]</sup> developed a bacteria-responsive coating that is able to be both antibacterial and cell-repellent. They have created a bilayer coating made of an inner layer of 2-vinyl-4,4-dimethyl azlactone loaded with an antimicrobial peptide (AMP) and an outer layer of PMAA. Under physiological conditions, the outer layer of PMAA limits bacterial adhesion to the surface and sequesters AMPs. When the local environment becomes acidic, PMAA chains dehydrate and collapse. Therefore, the local pH decrease occurring during infection will cause dehydration and retraction of the PMAA layer, which will expose the inner layer of AMP and kill bacteria on the surface. Once the pH becomes physiological, the layer of PMAA reforms a hydrated layer and switches between bactericidal to bacteria-repellent properties. The biggest advantage of this coating is that there is no need of additional reloading of new antibacterial agents to maintain its activity.

#### 4.2. Enzyme-triggered films

To be specific for a bacterial genus, Wang *et al.*<sup>[55]</sup> have designed a LbL film, which responded to two stimuli: enzymatic and pH. They built it by alternating 10 bilayers of PEG-bis(succinimidyl succinate) (NHS-PEG-NHS) and polyethylenimine (PEI) on cellulose substrates (noted as Cellulose<sub>LbL10</sub>), followed by immobilizing antibiotics *via* an acid-labile b-carboxylic linker and electrostatic adsorption of HA. The upper layer of HA provides good biocompatibility under normal physiological conditions. Release Van happens in two steps: degradation of the HA layer by HAase produced by Gram-positive bacteria and release of Van in response to the local bacteria-triggered acidification. Thus, degradation of the HA layer by HAase is necessary to allow the release of Van, which only occurs at pH 5.0. Therefore, as

shown in **Figure 14**, release of Van is more important at low pH (pH 5.0) than at medium pH (pH 7.4) for the Cellulose<sub>LbL10</sub>-Van coating.

The enzyme-responsive approach has been also exploited alone to reach effective antimicrobial coatings. Hence, Yao and co-workers<sup>[56]</sup> created a multilayer film built in two blocks and responding to the action of the HAase and CMS. The multilayer film is composed of 10 bilayers of HA/CH on which are added 10 bilayers of HA/ poly-L-lysine hydrobromide (PLL). They have shown that after 3 days and 6 days of incubation in HAase/CMS solution or in presence of *S. aureus*, respectively, the first block of (HA/PLL)<sub>10</sub> of a (HA/CH)<sub>10</sub>-(HA/PLL)<sub>10</sub> film was totally degraded. In the bottom (HA/CH)<sub>10</sub> multilayers films, CH prevented enzymatic degradation of HA by HAase through a blocking effect, thus allowing this bottom multilayer to provide a bactericidal function through contact-killing with the NH<sub>3</sub><sup>+</sup> groups of CH. Besides, degradation and subsequent detachment of fragments from the (HA/PLL)<sub>10</sub> film can reduce bacterial adhesion. *In vitro* test finally showed good bactericidal activity against *S. aureus* and *E. coli*, as well as good eukaryotic cell biocompatibility.

Diverse antimicrobial agents have been also used in coatings based on the enzyme-responsive strategy, including silver nanoparticles, antibiotics and antimicrobial peptides derived from human immune system. Liu *et al.*<sup>[57]</sup> have used a CH/HA multilayer film in combination with AgNPs. Nanocomposites formed with CH and AgNPs (CH@AgNPs) were synthesized using ascorbic acid as reducing agent and assembled with HA to obtain a (CH@AgNPs/HA)<sub>5</sub> coating. In contact with exogenous HAase, silver ions were rapidly released from the coating in the first 24 h, conferring it the expected antibacterial activity. Wang and co-workers<sup>[58]</sup> have elaborated two bacteria self-defensive LbL films by using GS as the antibacterial agent. The first one was made up of 8 bilayers of montmorillonite/poly-L-lysine-gentamicin sulfate ((MMT/PLL-GS)<sub>8</sub>) and the antibacterial activity was triggered by the action of CMS.<sup>[58a]</sup> The second one was made up of 10 bilayers of montmorillonite/hyaluronic acid-gentamicin sulfate ((MMT/HA-GS)<sub>10</sub>)

and the antibacterial activity was triggered by the action of HAase.<sup>[58b]</sup> In both cases, gradual degradation of the film by enzymes causes GS release from the matrix. Furthermore, peeling of the films from the surface leads to elimination of the fixed bacteria. Antibacterial activity tests revealed that both coatings allow good inhibition of biofilm formation and long-term anti-adhesive properties for *E. coli* and *S. aureus*. Francesko *et al.*<sup>[59]</sup> developed aminocellulose nanospheres (AC<sub>NSS</sub>)/HA multilayer films to fight against *P. aeruginosa*, a bacterial species widely found in medical devices-associated infections. The antibacterial agent here is aminocellulose in the form of nanospheres, which reveals better antibacterial activity than its counterpart in solution (AC<sub>sol</sub>). As shown in **Figure 15**, the AC<sub>NSS</sub>-based multilayer coatings (5 and 10 bilayers) reduced planktonic bacterial growth by about 70% after 2h incubation, whereas AC<sub>sol</sub>-based coatings affected bacterial cell growth by only 42%. This antibacterial activity of the coating was due to the release of AC<sub>NSS</sub> contained in the film, happening upon triggering of degradation of the coating by bacteria. For longer incubation times (7 days), the 10 bilayers film that contains the highest quantity of bioactive agent, proved to be the most effective against biofilm formation by *P. aeruginosa*. Cado *et al.*<sup>[60]</sup> have developed a LbL-based enzyme-responsive coating with an antimicrobial peptide, cateslytin (CTL), as the active agent. A biocompatible and biodegradable polysaccharide multilayer film consisting of hyaluronic acid functionalized with an CTL, and CH was built. The authors showed that *S. aureus* and *C. albicans*, two pathogens secreting hyaluronidase, were able to degrade HA/CH film by hydrolysis of HA. The films composed of 15 bilayers (HA-CTL/CH)<sub>15</sub> even completely inhibited growth of both pathogens after 24 h of incubation. Thanks to the fluorescent labeling of HA (HA<sup>FITC</sup>) and HA-CTL (HA<sup>FITC</sup>-CTL) chains, the interaction of both molecules with *C. albicans* was demonstrated. HA<sup>FITC</sup>-CTL fragments were detectable in cytoplasm without inducing cell lysis, whereas HA<sup>FITC</sup> was found only around yeast cells. This suggests that CTL



was able to cross microbial cell membrane, even when linked to HA, thus inducing the cell death.

Finally, many systems have already been developed with the common aim to trigger the antimicrobial properties through an infection-based stimulus. All of those presented above reached this goal, thus clearly demonstrating this ambitious concept. They varied in the strategy used to trigger the antimicrobial activity, which was induced either by variation in pH or enzyme, but they all successfully exploited the microbial cells present at the infection site as the initial effector. Thus, in the absence of microorganisms, leakage of antimicrobial molecules into the material environment, or even contact of them with the external tissues when contact-killing effect on microorganisms rather than release is expected, is avoided. This strict drug confinement in absence of infection should reduce side effects of the drugs on normal tissues and more broadly, limit systemic exposure of the patient.

Nevertheless, several aspects are still to be examined in the field of infection-responsive smart coatings. In particular, their performances and mechanisms of action in *in vivo* conditions are only sparsely known. For most of them, no *in vivo* evaluation has been reported so far. Bu *et al* [27c] and Zhou *et al*[34] have already shown the ability of their coatings to inhibit bacterial growth *in vivo* but dose-dependent effects and comparison to systemic administration have not been extensively studied. In other words, it has not been completely proven whether these systems can provide earlier action, more specific and better dosing in real conditions of use than more conventional antimicrobial coatings. In addition, reduction of the side effects related to local versus systemic exposures has not been proven so far. Moreover, low biocompatibility and potential toxicity may result from the release of polymer fragments due to the pH- or enzyme-induced degradation, which may induce inflammatory or toxic response, or prevent adhesion of mammalian cells. Integration of such smart coatings in patients' body must be therefore now investigated to confirm their real potential for application on medical devices. Varying the

coating matrix may also pave the way to new systems, since only few different polymers and the associated enzymes have been exploited until now. HA and hyaluronidase have been by far the most frequently used. Finally, to further limit the dispersion in patient body of antimicrobial agents which are potentially toxic molecules, the idea may now emerge to change the nature of the final effector: next step may be now to early trigger the patient's immune system as a response to the early detection of the infection by the coating.

## **5. Conclusion**

To fight against antibiotic-resistant bacteria adhering and developing on medical devices, which is a growing problem worldwide, researchers are currently developing new “smart” materials and coatings. Such systems allow to control drug release depending on the absence/presence of infection, thus localizing the treatment area and avoiding drug dilution to healthy tissues.

In this review, we described three classes of innovative materials: hydrogels, nanomaterials and thin films. Moreover, smart antibacterial coatings can be classified into two groups: those that respond to a non-biological stimulus (light, temperature, electric and magnetic fields) and those that respond to a biological stimulus related to the presence of bacteria, such as changes in pH or bacterial enzyme secretion. Among the described systems, pH-responsive smart materials are the most popular, and most of them respond to acidification. However, pH does not vary in the same way from one tissue to another, thus the intended application of the coating must be considered when using pH as a triggering stimulus for antibacterial activity.

In this context, bacterial enzyme-triggered systems are very promising. Such systems, while remaining passive in the absence of infection, are activated by the bacteria themselves, and this is independent of the pH.

In addition, some stimulus-triggered smart systems are designed in a way to have anti-adhesive properties, to prevent bacterial adhesion and biofilm formation. This is their great advantage, because biofilms are very difficult to eradicate.

Of note, layer-by-layer deposition method, due to its versatility, appears to be extremely efficient for elaboration of complex responsive systems. Multilayer films can be composed of many different components (antibacterial agents, polymers that limit bacterial adhesion, pH-responsive polymers, Ag nanoparticles), making them truly multifunctional and smart and their production on medical device is easy to scale-up.

## **Acknowledgements**

This project has received funding from the European Union's Horizon 2020 PANBioRA research and innovation program under grant agreement no. 760921 and from the European Regional Development Fund (ERDF) in the framework of the INTERREG V Upper Rhine program “Transcending borders with every project”, project NANOTRANSMED.

Received: ((will be filled in by the editorial staff))

Revised: ((will be filled in by the editorial staff))

Published online: ((will be filled in by the editorial staff))

**References**

- [1] European Centre for Disease Prevention and Control, Annual report of the European Antimicrobial Resistance - Surveillance Network (EARS-Net) 2017, 2018
- [2] WHO, Antimicrobial resistance: global report on surveillance 2014, <https://www.who.int/drugresistance/documents/surveillancereport/en/>, April 2014
- [3] C. f. D. C. a. Prevention, Antibiotic Resistance Threats in the United States 2013, <http://www.cdc.gov/drugresistance/threat-report-2013/>, 2016
- [4] J. O'Neill, Review on Antimicrobial Resistance. Securing New Drugs for Future Generations: The Pipeline of Antibiotics, [http://amr-review.org/sites/default/files/SECURING%20NEW%20DRUGS%20FOR%20FUTURE%20GENERATIONS%20FINAL%20WEB\\_0.pdf](http://amr-review.org/sites/default/files/SECURING%20NEW%20DRUGS%20FOR%20FUTURE%20GENERATIONS%20FINAL%20WEB_0.pdf), May 2015
- [5] J. A. Ayukekbong, M. Ntemgwa, A. N. Atabe, *Antimicrob Resist In* **2017**, 6, 47.
- [6] R. M. Donlan, J. W. Costerton, *Clin. Microbiol. Rev.* **2002**, 15, 167.
- [7] Z. Khatoon, C. D. McTiernan, E. J. Suuronen, T. F. Mah, E. I. Alarcon, *Heliyon* **2018**, 4, e01067.
- [8] M. Wang, T. Tang, *J Orthop Translat* **2019**, 17, 42.
- [9] a) J. W. Costerton, P. S. Stewart, E. P. Greenberg, *Science* **1999**, 284, 1318; b) A. J. Huh, Y. J. Kwon, *J. Controlled Release* **2011**, 156, 128.
- [10] A. W. Smith, *Adv. Drug Deliv. Rev.* **2005**, 57, 1539.
- [11] G. Schmidmaier, M. Lucke, B. Wildemann, N. P. Haas, M. Raschke, *Injury* **2006**, 37, 105.
- [12] a) C. T. Gustafson, F. Boakye-Agyeman, C. L. Brinkman, J. M. Reid, R. Patel, Z. Bajzer, M. Dadsetan, M. J. Yaszemski, *Plos One* **2016**, 11, 17; b) J. S. Patton, C. S. Fishburn, J. G. Weers, *Proc. Am. Thorac. Soc.* **2004**, 1, 338.

- [13] a) D. Y. Cho, D. J. Lim, C. Mackey, C. G. Weeks, J. A. P. Garcia, D. Skinner, S. Zhang, J. McCormick, B. A. Woodworth, *Int. Forum Allergy Rhinol.* **2019**, 9, 486; b) M. Stigter, J. Bezemer, K. de Groot, P. Layrolle, *J. Controlled Release* **2004**, 99, 127.
- [14] A. E. Pérez-Cobas, A. Artacho, H. Knecht, M. L. Ferrús, A. Friedrichs, S. J. Ott, A. Moya, A. Latorre, M. J. Gosalbes, *Plos One* **2013**, 8, e80201.
- [15] a) G. Gao, Y. W. Jiang, H. R. Jia, F. G. Wu, *Biomaterials* **2019**, 188, 83; b) Q. Liu, L. Liu, *Langmuir* **2019**, 35, 1450; c) Q. Chen, C. Zhu, D. Huo, J. Xue, H. Cheng, B. Guan, Y. Xia, *Nanoscale* **2018**, 10, 22312; d) Z. Y. Song, Y. Wu, Q. Cao, H. J. Wang, X. R. Wang, H. Y. Han, *Adv. Funct. Mater.* **2018**, 28; e) Y. Xie, S. Chen, Y. Qian, W. Zhao, C. Zhao, *Mater. Sci. Eng., C* **2018**, 84, 52; f) D. Gabriel, I. P. Monteiro, D. Huang, R. Langer, D. S. Kohane, *Biomaterials* **2013**, 34, 9763.
- [16] a) O. Werzer, S. Tumphart, R. Keimel, P. Christian, A. M. Coclite, *Soft Matter* **2019**; b) Y. Pan, B. Li, Z. Liu, Z. Yang, X. Yang, K. Shi, W. Li, C. Peng, W. Wang, X. Ji, *ACS Appl Mater Inter* **2018**, 10, 32747; c) O. Zavgorodnya, C. A. Carmona-Moran, V. Kozlovskaya, F. Liu, T. M. Wick, E. Kharlampieva, *J. Colloid Interface Sci.* **2017**, 506, 589; d) M. G. Arafa, R. F. El-Kased, M. M. Elmazar, *Sci. Rep.* **2018**, 8, 13674; e) H. T. Yang, G. F. Li, J. W. Stansbury, X. Q. Zhu, X. Wang, J. Nie, *ACS Appl Mater Inter* **2016**, 8, 28047; f) G. A. Islan, P. C. Tornello, G. A. Abraham, N. Duran, G. R. Castro, *Colloids Surf. B* **2016**, 143, 168; g) B. Wang, Q. Xu, Z. Ye, H. Liu, Q. Lin, K. Nan, Y. Li, Y. Wang, L. Qi, H. Chen, *ACS Appl Mater Inter* **2016**, 8, 27207; h) A. S. Kritchenkov, A. R. Egorov, N. V. Dubashynskaya, O. V. Volkova, L. A. Zabodalova, E. P. Suchkova, A. V. Kurliuk, T. V. Shakola, A. P. Dysin, *Int. J. Biol. Macromol.* **2019**.
- [17] a) E. L. Silva-Freitas, T. R. F. Pontes, R. P. Araujo-Neto, A. H. M. Damasceno, K. L. Silva, J. F. Carvalho, A. C. Medeiros, R. B. Silva, A. K. A. Silva, M. A. Morales, E. S. T.

- Egito, A. L. Dantas, A. S. Carrico, *AAPS PharmSciTech* **2017**, 18, 2026; b) J. Qu, X. Zhao, P. X. Ma, B. Guo, *Acta Biomater.* **2018**, 72, 55.
- [18] a) L. Zhang, Y. Wang, J. Wang, Y. Wang, A. Chen, C. Wang, W. Mo, Y. Li, Q. Yuan, Y. Zhang, *ACS Appl Mater Inter* **2018**; b) L. Zhang, Y. Wang, J. Wang, Y. Wang, A. Chen, C. Wang, W. Mo, Y. Li, Q. Yuan, Y. Zhang, *ACS Appl Mater Inter* **2019**, 11, 300.
- [19] a) P. Rathi, S. Bradoo, R. K. Saxena, R. Gupta, *Biotechnol. Lett* **2000**, 22, 495; b) W. L. Hynes, S. L. Walton, *FEMS Microbiol. Lett.* **2000**, 183, 201; c) L. Shaw, E. Golonka, J. Potempa, S. J. Foster, *Microbiol-Sgm* **2004**, 150, 217.
- [20] B. Skalka, *Vet. Med. (Praha)* **1985**, 30, 373.
- [21] a) J. M. Vroom, K. J. De Grauw, H. C. Gerritsen, D. J. Bradshaw, P. D. Marsh, G. K. Watson, J. J. Birmingham, C. Allison, *Appl. Environ. Microbiol.* **1999**, 65, 3502; b) M. Hannig, C. Hannig, *Nat. Nanotechnol.* **2010**, 5, 565; c) G. Hidalgo, A. Burns, E. Herz, A. G. Hay, P. L. Houston, U. Wiesner, L. W. Lion, *Appl. Environ. Microbiol.* **2009**, 75, 7426.
- [22] L. A. Schneider, A. Korber, S. Grabbe, J. Dissemond, *Arch Dermatol Res* **2007**, 298, 413.
- [23] G. Gethin, *The significance of surface pH in chronic wounds*, Vol. 3, 2007.
- [24] V. Albright, I. Zhuk, Y. Wang, V. Selin, B. van de Belt-Gritter, H. J. Busscher, H. C. van der Mei, S. A. Sukhishvili, *Acta Biomater.* **2017**, 61, 66.
- [25] Q. B. Wei, F. Fu, Y. Q. Zhang, L. Tang, *J. Polym. Res.* **2014**, 21.
- [26] J. Zhou, S. Hou, L. H. Li, D. Y. Yao, Y. Y. Liu, A. T. A. Jenkins, Y. B. Fan, *Adv. Mater.* **2018**, 5.
- [27] a) J. Hu, Y. Quan, Y. Lai, Z. Zheng, Z. Hu, X. Wang, T. Dai, Q. Zhang, Y. Cheng, *J. Controlled Release* **2017**, 247, 145; b) T. Dai, C. Wang, Y. Wang, W. Xu, J. Hu, Y. Cheng, *ACS Appl Mater Inter* **2018**, 10, 15163; c) Y. Bu, L. Zhang, J. Liu, L. Zhang, T. Li, H. Shen, X. Wang, F. Yang, P. Tang, D. Wu, *ACS Appl Mater Inter* **2016**, 8, 12674.

- [28] a) M. Li, H. Wang, J. Hu, J. Hu, S. Zhang, Z. Yang, Y. Li, Y. Cheng, *Chem. Mater.* **2019**, 31, 7678; b) J. Hu, Q. Hu, X. He, C. Liu, Y. Kong, Y. Cheng, Y. Zhang, *Adv. Healthc. Mater.* **2020**, 9, 1901329; c) J. Hu, Z. Zheng, C. Liu, Q. Hu, X. Cai, J. Xiao, Y. Cheng, *Biomater. Sci.* **2019**, 7, 581; d) H. Wang, Y. Cheng, *Mater. Chem. Front.* **2019**, 3, 472.
- [29] X. Cheng, M. Li, H. Wang, Y. Cheng, *Chin. Chem. Lett.* **2020**, 31, 869.
- [30] P. Wang, K. L. Tan, E. T. Kang, K. G. Neoh, *J. Membr. Sci.* **2002**, 195, 103.
- [31] A. Hassan, M. B. K. Niazi, A. Hussain, S. Farrukh, T. Ahmad, *J. Polym. Environ.* **2018**, 26, 235.
- [32] M. E. Villanueva, M. L. Cuestas, C. J. Perez, V. C. Dall'Orto, G. J. Copello, *J. Colloid Interface Sci.* **2019**, 536, 372.
- [33] J. Zhu, H. Han, T. T. Ye, F. X. Li, X. L. Wang, J. Y. Yu, D. Q. Wu, *Molecules* **2018**, 23, 15.
- [34] J. Zhou, D. Yao, Z. Qian, S. Hou, L. Li, A. T. A. Jenkins, Y. Fan, *Biomaterials* **2018**, 161, 11.
- [35] F. B. Zeynabad, R. Salehi, E. Alizadeh, H. S. Kafil, A. M. Hassanzadeh, M. Mahkam, *Rsc Adv.* **2015**, 5, 105678.
- [36] E. Montanari, A. Gennari, M. Pelliccia, C. Gourmel, E. Lallana, P. Matricardi, A. J. McBain, N. Tirelli, *Macromol. Biosci.* **2016**, 16, 1815.
- [37] K. R. Sims, Y. Liu, G. Hwang, H. I. Jung, H. Koo, D. S. W. Benoit, *Nanoscale* **2018**, 11, 219.
- [38] D. Y. Zhu, R. F. Landis, C. H. Li, A. Gupta, L. S. Wang, Y. Geng, S. Gopalakrishnan, J. W. Guo, V. M. Rotello, *Nanoscale* **2018**, 10, 18651.
- [39] Z. Liu, Y. Zhu, X. Liu, K. W. K. Yeung, S. Wu, *Colloids Surf. B* **2017**, 151, 165.
- [40] D. Pornpattananangkul, L. Zhang, S. Olson, S. Aryal, M. Obonyo, K. Vecchio, C. M. Huang, L. F. Zhang, *J. Am. Chem. Soc.* **2011**, 133, 4132.

- [41] M. Fraunholz, B. Sinha, *Front. Cell Infect. Microbiol.* **2012**, 2.
- [42] S. Yang, X. Han, Y. Yang, H. Qiao, Z. Yu, Y. Liu, J. Wang, T. Tang, *ACS Appl Mater Inter* **2018**, 10, 14299.
- [43] M.-H. Xiong, Y. Bao, X.-Z. Yang, Y.-C. Wang, B. Sun, J. Wang, *J. Am. Chem. Soc.* **2012**, 134, 4355.
- [44] N. Takahashi, B. Nyvad, *J. Dent. Res* **2011**, 90, 294.
- [45] C. A. Stewart, J. H. Hong, B. D. Hatton, Y. Finer, *Acta Biomater.* **2018**, 76, 283.
- [46] P. C. Nalam, H. S. Lee, N. Bhatt, R. W. Carpick, D. M. Eckmann, R. J. Composto, *ACS Appl Mater Inter* **2017**, 9, 12936.
- [47] H. S. Lee, S. S. Dastgheyb, N. J. Hickok, D. M. Eckmann, R. J. Composto, *Biomacromolecules* **2015**, 16, 650.
- [48] B. Wang, H. Liu, Z. Wang, S. Shi, K. Nan, Q. Xu, Z. Ye, H. Chen, *J. Mater. Chem. B* **2017**, 5, 1498.
- [49] H. Chen, Z. Ye, L. Sun, X. Li, S. Shi, J. Hu, Y. Jin, Q. Xu, B. Wang, *Carbohydr. Polym.* **2018**, 189, 65.
- [50] L. Sutrisno, S. Wang, M. Li, Z. Luo, C. Wang, T. Shen, P. Chen, L. Yang, Y. Hu, K. Cai, *J. Mater. Chem. B* **2018**, 6, 5290.
- [51] S. Pavlakhina, I. Zhuk, A. Mentbayeva, E. Rautenberg, W. Chang, X. Yu, B. van de Belt-Gritter, H. J. Busscher, H. C. van der Mei, S. A. Sukhishvili, *Npg Asia Mater.* **2014**, 6, e121.
- [52] I. Zhuk, F. Jariwala, A. B. Attygalle, Y. Wu, M. R. Libera, S. A. Sukhishvili, *ACS Nano* **2014**, 8, 7733.
- [53] J. Yan, W. Zhou, Z. Jia, P. Xiong, Y. Li, P. Wang, Q. Li, Y. Cheng, Y. Zheng, *Acta Biomater.* **2018**, 79, 216.



- [54] S. J. Yan, H. C. Shi, L. J. Song, X. H. Wang, L. Liu, S. F. Luan, Y. M. Yang, J. H. Yin, *ACS Appl Mater Inter* **2016**, 8, 24471.
- [55] X. H. Wang, L. J. Song, J. Zhao, R. T. Zhou, S. F. Luan, Y. B. Huang, J. H. Yin, A. Khan, *J. Mater. Chem. B* **2018**, 6, 7710.
- [56] Q. Yao, Z. Ye, L. Sun, Y. Jin, Q. Xu, M. Yang, Y. Wang, Y. Zhou, J. Ji, H. Chen, B. Wang, *J. Mater. Chem. B* **2017**, 5, 8532.
- [57] P. Liu, Y. Hao, Y. Ding, Z. Yuan, Y. Liu, K. Cai, *J. Mater. Sci.: Mater. Med.* **2018**, 29, 160.
- [58] a) Q. Xu, X. Li, Y. Jin, L. Sun, X. Ding, L. Liang, L. Wang, K. Nan, J. Ji, H. Chen, B. Wang, *Nanoscale* **2017**, 9, 19245; b) B. Wang, H. Liu, L. Sun, Y. Jin, X. Ding, L. Li, J. Ji, H. Chen, *Biomacromolecules* **2018**, 19, 85.
- [59] A. Francesko, M. M. Fernandes, K. Ivanova, S. Amorim, R. L. Reis, I. Pashkuleva, E. Mendoza, A. Pfeifer, T. Heinze, T. Tzanov, *Acta Biomater.* **2016**, 33, 203.
- [60] G. Cado, R. Aslam, L. Séon, T. Garnier, R. Fabre, A. Parat, A. Chassepot, J.-C. Voegel, B. Senger, F. Schneider, Y. Frère, L. Jierry, P. Schaaf, H. Kerdjoudj, M.-H. Metz-Boutigue, F. Boulmedais, *Adv. Funct. Mater.* **2013**, 23, 4801.
- [61] S. Pavlukhina, Y. Lu, A. Patimetha, M. Libera, S. Sukhishvili, *Biomacromolecules* **2010**, 11, 3448.

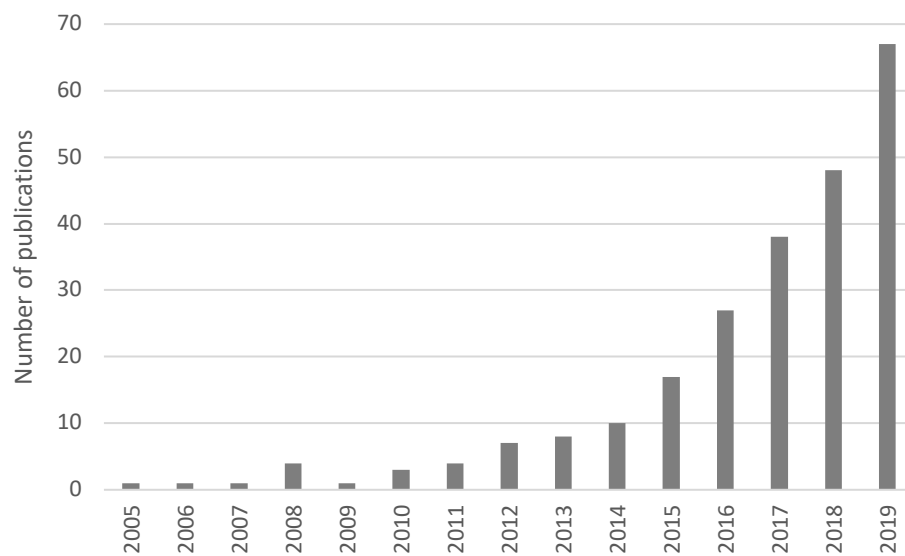


**Figure 1.** Total publications by year obtained on the basis of the following key words: "smart", "antibacterial", "surface".

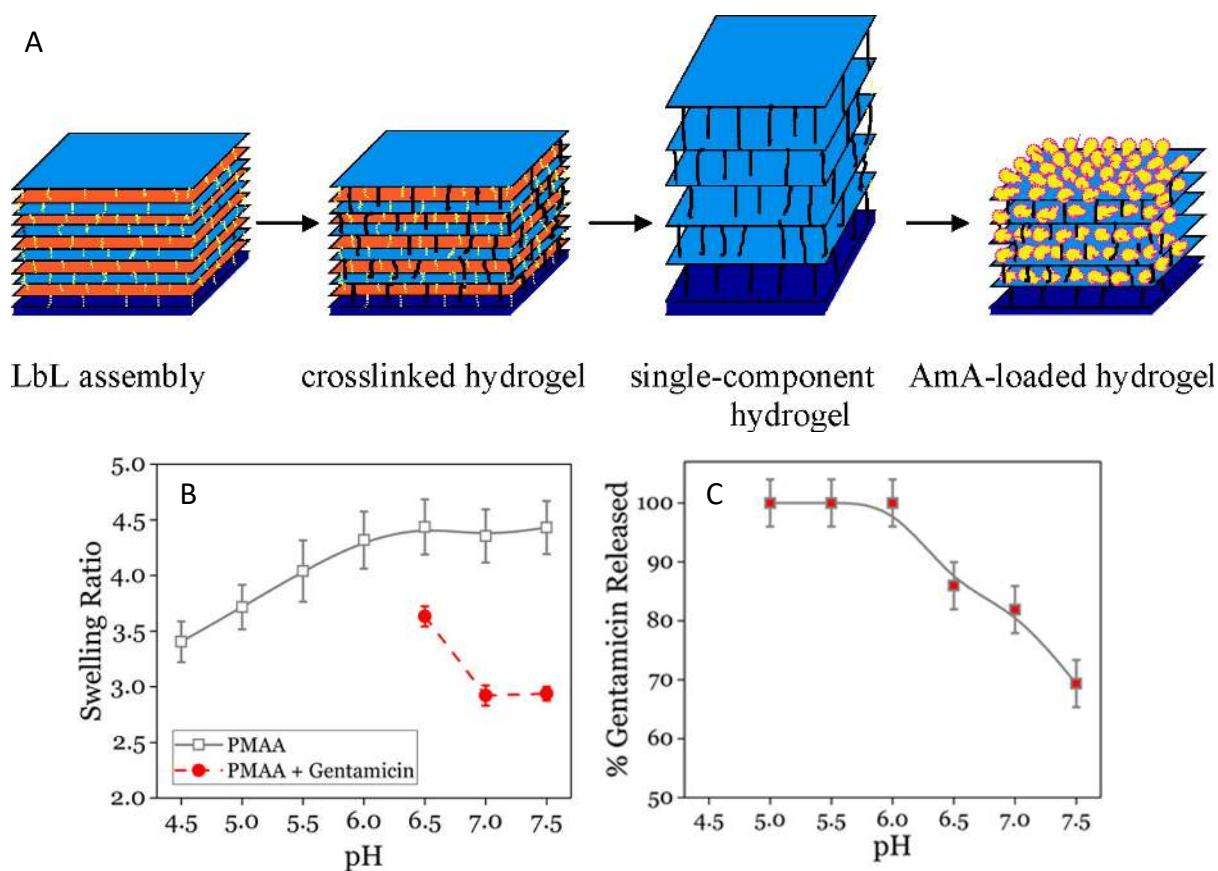


**Figure 2.** Procedure for preparation of PMAA-gentamicin loaded hydrogel (A). Copyright [61]. In situ ellipsometry data for the swelling ratios for unloaded and gentamicin-loaded 18-layer PMAA coatings in PBS as a function of pH (B) and percentage gentamicin released as measured by decrease in dry film thickness using ellipsometry after sequential 2 h exposures of the coatings to PBS with decreasing pH (C). Reproduced with permission<sup>[24]</sup> Copyright 2017, Elsevier.

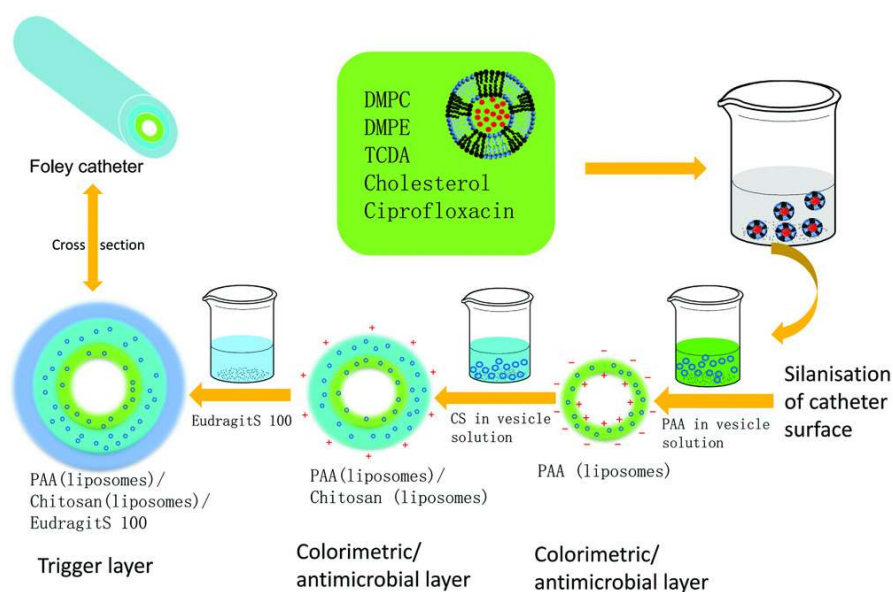


**Figure 3.** Schematic illustration of multilayer polymer on catheter surface by electrostatic self-assembly technique. PDA vesicles embedded in colorimetric layer and sealed by an outer layer of pH sensitivity. Reproduced with permission<sup>[26]</sup> Copyright 2018, Wiley.

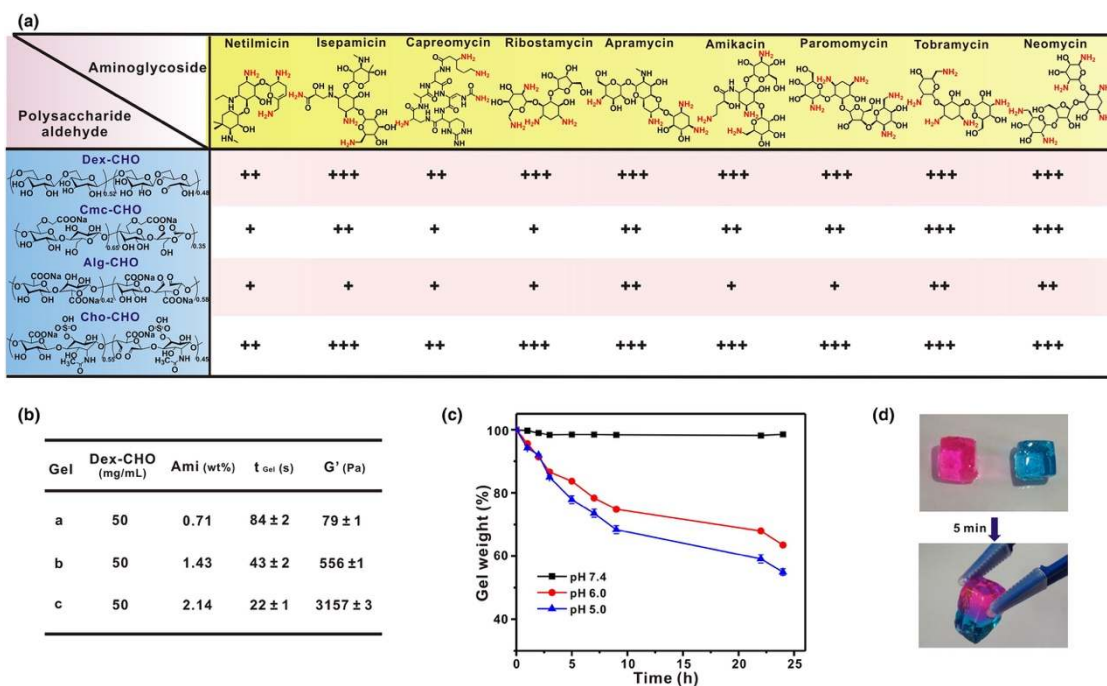


**Figure 4.** Properties of aminoglycoside hydrogels. (a) Gel formation between nine aminoglycosides and four types of polysaccharide aldehydes (dextran aldehyde (Dex-CHO); chondroitin aldehyde (Cho-CHO); carboxymethyl cellulose aldehyde (Cmc-CHO); alginate aldehyde (Alg-CHO)). “+”, “++”, and “+++” indicate the hydrogel forms within 15 min, 5 min, and 1 min, respectively. (b) Storage modulus and gelation time of amikacin/Dex-CHO hydrogels with different amikacin contents. (c) Degradation of the amikacin/Dex-CHO hydrogel (1.43 wt% amikacin) under pH 7.4, 6.0 and 5.0, respectively. (d) Self-healing behavior of the amikacin/Dex-CHO hydrogel. The two pieces of cube-shaped hydrogels were encapsulated with rhodamine B and methylene blue, respectively. Reproduced with permission.<sup>[27a]</sup> Copyright 2018, Wiley.

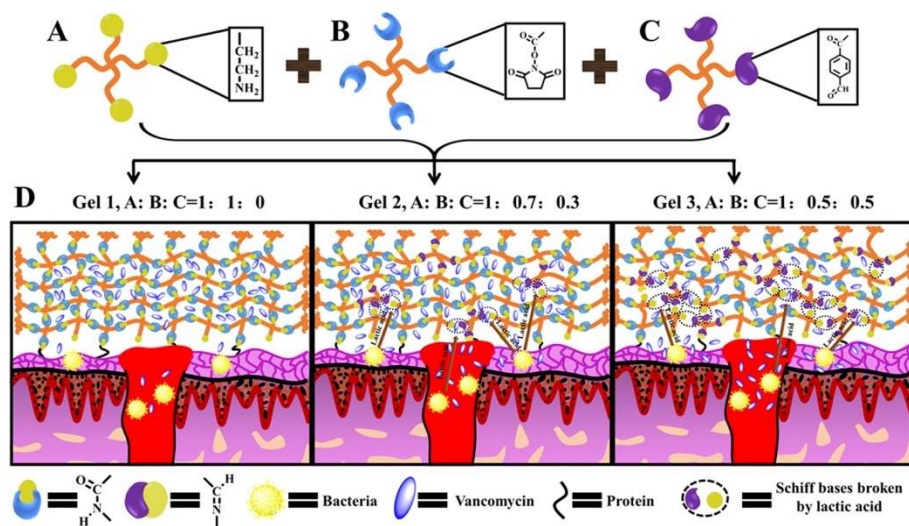


**Figure 5.** Vancomycin-loaded hydrogel systems formed by (A) 4-Arm-PEG-NH<sub>2</sub> reacting with (B) 4-Arm-PEG-NHS, (C) 4-Arm-PEG-CHO, and (D) polymer networks composed of different molar ratios of A: B: C, their adhesion to tissues and bacteria-responsive release of vancomycin. Reproduced with permission.<sup>[27c]</sup> Copyright 2018, Wiley.

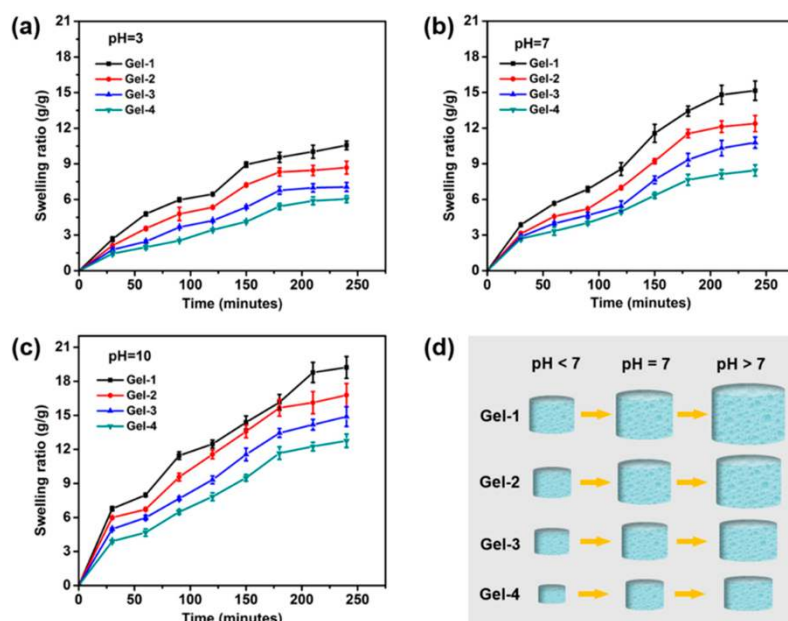


**Figure 6.** Swelling ratios of Gel-1 (black line), Gel-2 (red line), Gel-3 (blue line) and Gel-4 (green line) hydrogels at pH = 3 (a), pH = 7 (b) and pH = 10 (c) as a function of time. For gel production, the ratio of peptide-based bis-acrylate to AAC increasing from Gel 1 to Gel 4. (d) The trend of swelling vs hydrogels at pH = 3 (a), pH = 7 (b) and pH = 10 (c) as a function of time. (d) The trend of swelling vs pH of each hydrogel. The swelling ratio will increase when the solution became alkaline. Reproduced with permission.<sup>[33]</sup> Copyright 2018, Wiley.

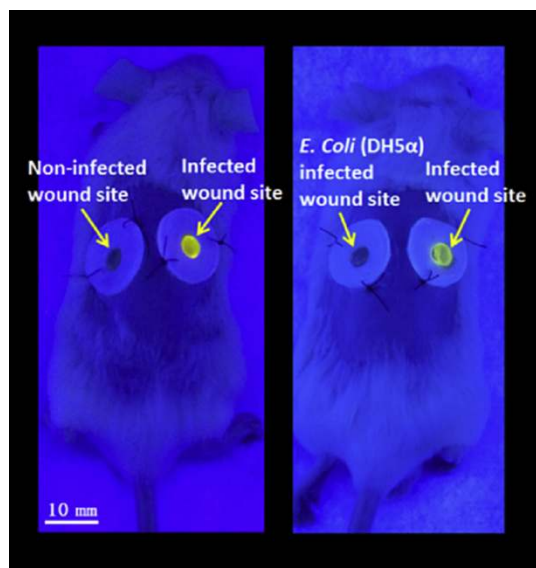


**Figure 7.** Representative imaging of colorimetric sensing property of the prototype wound dressing after 2-day surgery in Balb/c model. Non-infected wound site: blank control; infected wound site: *S. aureus* and *P. aeruginosa* of  $5.10^8$  CFU.mL<sup>-1</sup> inoculated on the wound site; *E. coli* (DH5a) infected wound site: *E. coli* (DH5a) of  $5.10^8$  CFU.mL<sup>-1</sup> inoculated on wound site. Reproduced with permission.<sup>[34]</sup> Copyright 2018, Wiley.



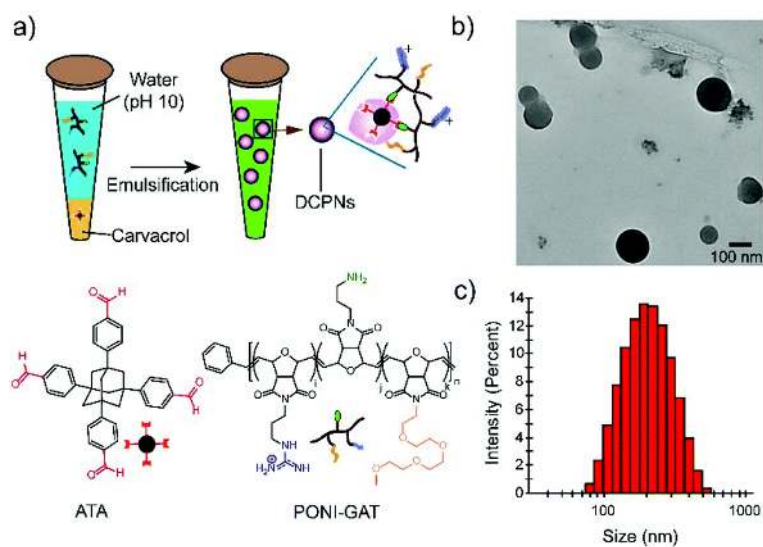


**Figure 8.** a) Schematic depiction of the strategy used to generate DCPNs along with the chemical structures of ATA crosslinker and PONI-GAT; b) TEM micrograph of DCPNs. Scale bar is 100 nm; c) DLS histogram indicating the size distribution of DCPNs in phosphate buffer saline (PBS, 150 mM). Reproduced with permission.<sup>[38]</sup> Copyright 2018, Wiley.

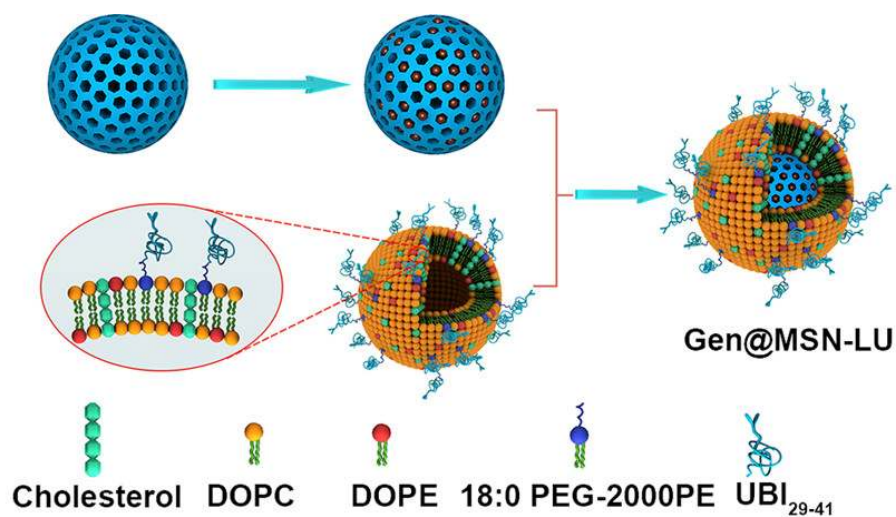


**Figure 9.** Schematics of the synthetic route of Gen@MSN-LU. UBI<sub>29-41</sub> was used to target the bacteria, and the outer layer of liposomes can be degraded by the bacterium-secreted toxins, leading to the Gen release. Reproduced with permission.<sup>[42]</sup> Copyright 2018, Wiley.

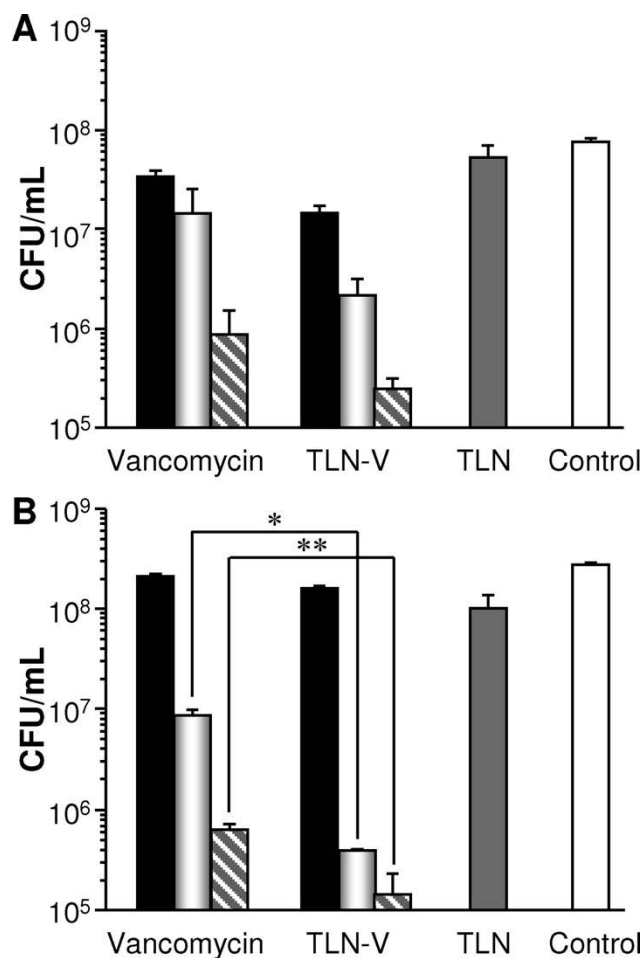


**Figure 10.** Intracellular survival of *S. aureus* MW2 in Raw264.7 cells. Infected cells were cultured with vancomycin, TLN-V, or empty TLN ( $476.2 \mu\text{g.mL}^{-1}$ , equal to the concentration of TLN in culture that the cells were treated with TLN-V at a vancomycin concentration of  $20 \mu\text{g.mL}^{-1}$ ) or left untreated (control). The final concentration of vancomycin in the culture was  $5$  (solid bar),  $10$  (gray bar), or  $20$  (striped bar)  $\mu\text{g.mL}^{-1}$  when it was applied. The incubation was terminated after 12 h (A) or 24 h (B) to determine the intracellular survival of *S. aureus*. CFU, colony-forming units. \* represents  $p < 0.05$  and \*\* represents  $p < 0.01$  determined by Student's t test. Reproduced with permission<sup>[43]</sup> Copyright 2018, Wiley.

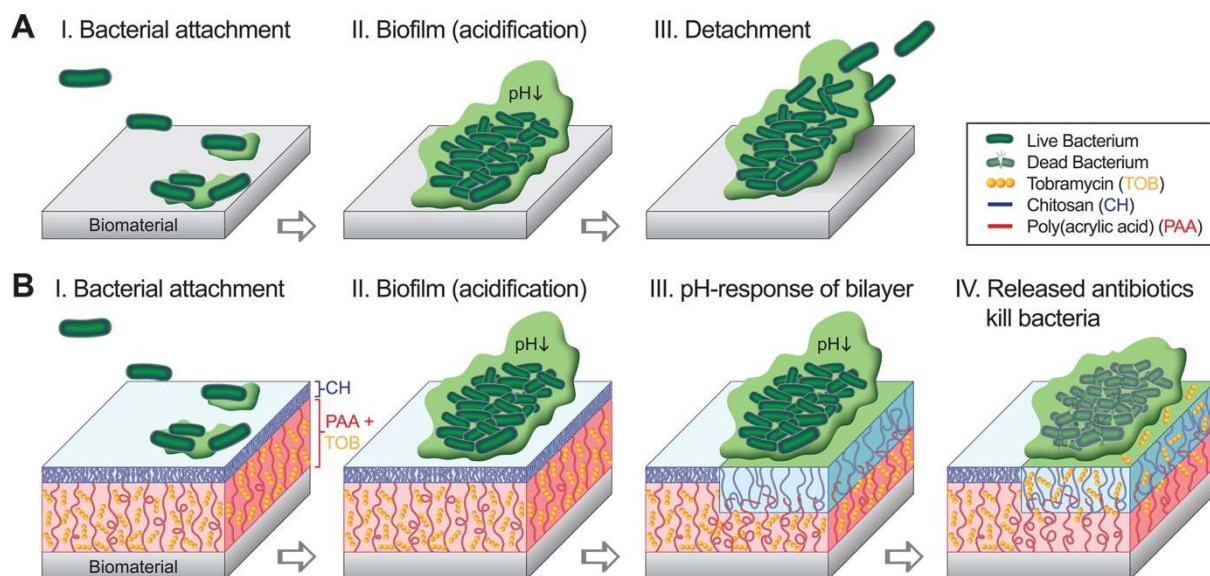


**Figure 11.** (A) Bacterial infection on biomaterials involves (I) bacterial attachment, (II) bacterial colonization and biofilm formation, and (III) biofilm detachment for bacterial proliferation. (B) pH-responsive, drug release polymer bilayer system has an outer layer of chitosan (CH, blue), which provides biocompatibility and hemocompatibility. This layer minimizes blood coagulation and inflammation when a biomaterial comes in direct contact with biological tissue and provides initial resistance against bacterial infection. An inner layer of poly(acrylic acid) (PAA, red) is grown from the biomaterial using surface-initiated atomic transfer radical polymerization (SI-ATRP). The molecular weight can be varied to tune the loading amount of tobramycin (TOB, yellow), which is electrostatically attracted to the PAA at pH 7. The depicted drug release mechanism is that bacterial colonization and formation of a biofilm on the TOB-loaded CH/PAA bilayer causes a local decrease in pH near the infected area (B.II). The reduced local pH triggers the outer CH layer to swell and reduces the electrostatic attraction between PAA and TOB (B.III). TOB loaded in PAA releases and diffuses into biofilm to kill the bacteria (B.IV). In summary, TOB is loaded at pH ~4.5, retained at pH 7 and released at low pH. Reproduced with permission.<sup>[47]</sup> Copyright 2018, Wiley.

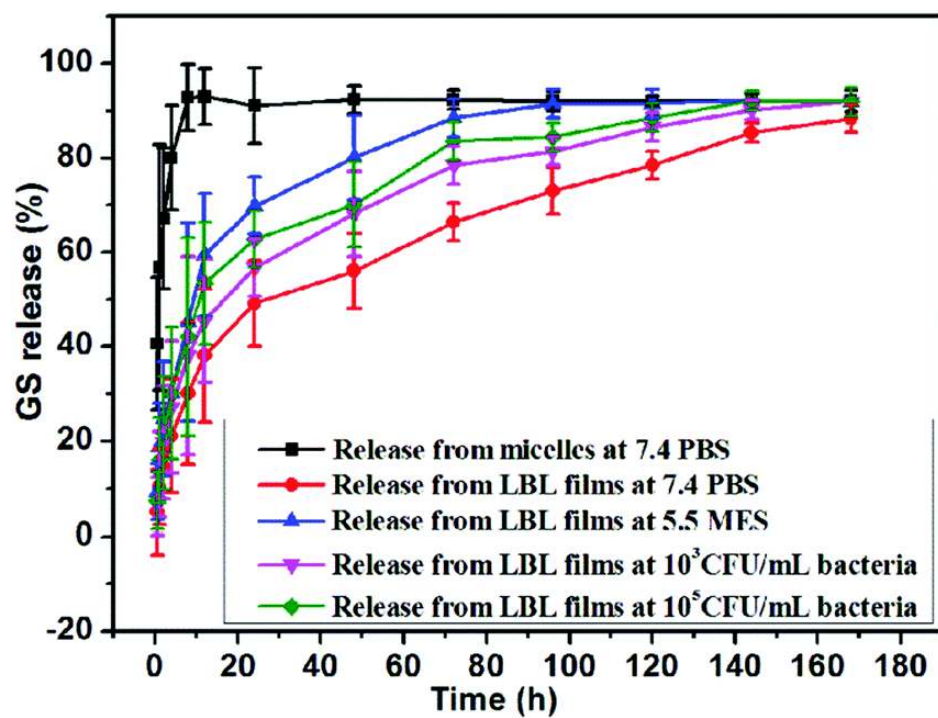


**Figure 12.** Normalized cumulative TCA release from (TCA/MPEG-PCL-CS)/PAA multilayer films in different medium. Reproduced with permission.<sup>[48]</sup> Copyright 2018, Wiley.

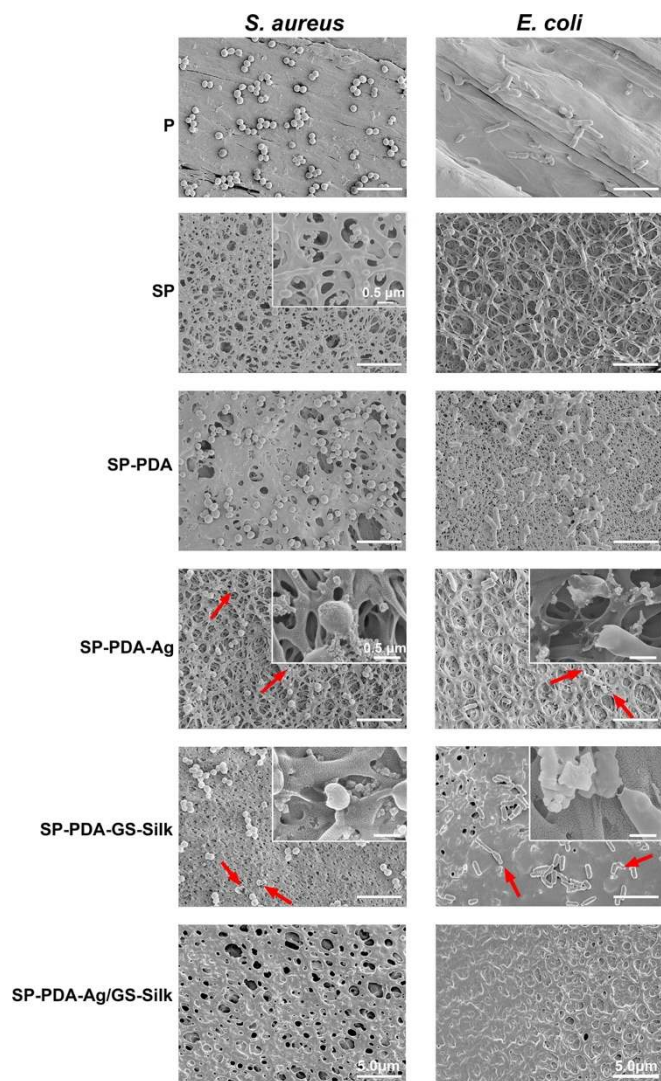


**Figure 13.** SEM morphology of bacteria adhered to the surfaces after incubated with samples for 24 h, and high magnification images of bacteria adhered to SP sample or bacteria damaged were inserted on the upper right corner. Red arrows indicate bacteria with impaired structure. Reproduced with permission.<sup>[53]</sup> Copyright 2018, Wiley.

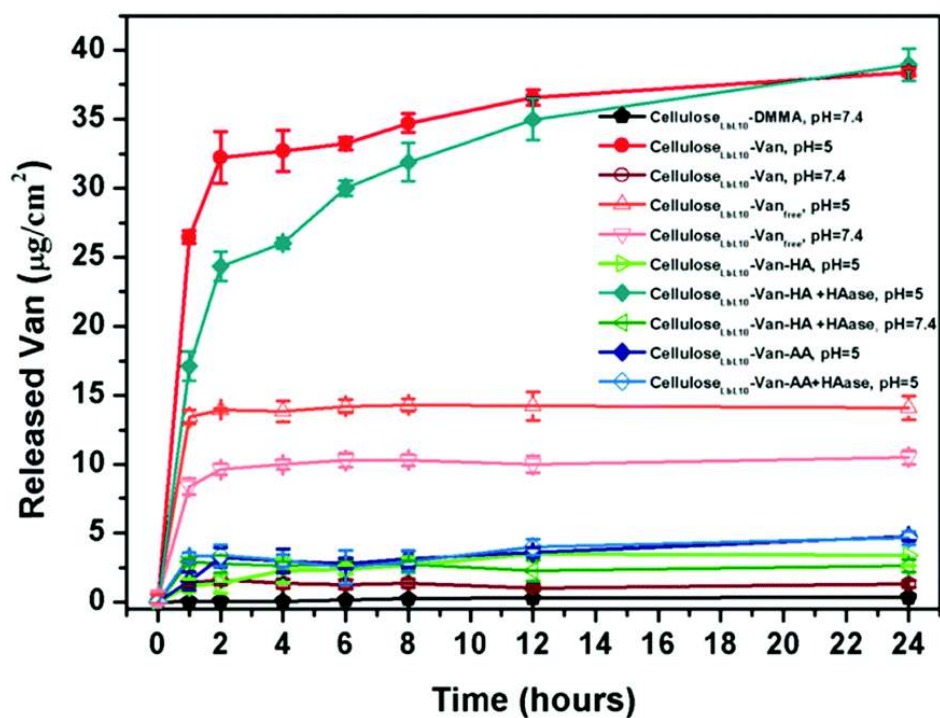


**Figure 14.** Time-dependent release profile of Van under different conditions. (Error bars: standard deviation,  $n = 3$ ). Reproduced with permission.<sup>[55]</sup> Copyright 2018, Wiley.

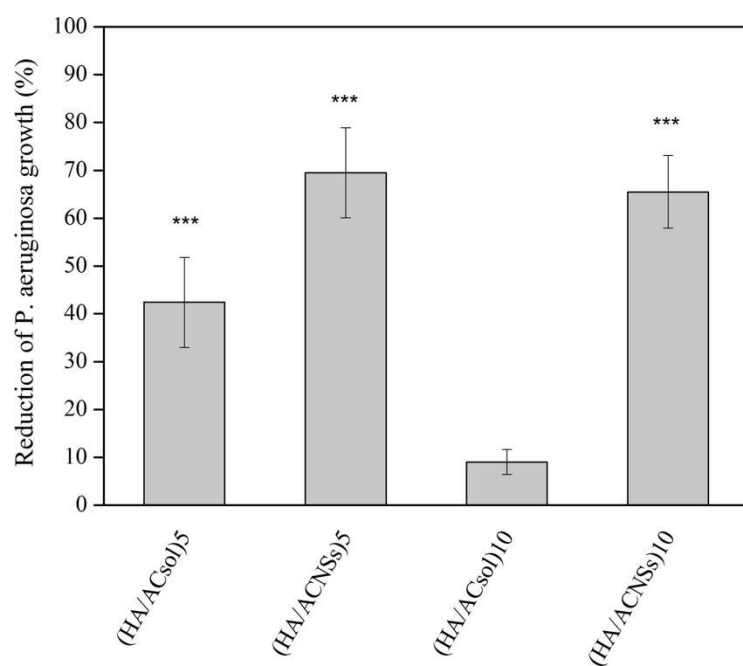


**Figure 15.** Antibacterial activity of silicone coated with HA/ACsol and HA/ACNSs against *P. aeruginosa* as compared to pristine silicone. Statistical differences are represented as \*\*\* $p < 0.001$ . Reproduced with permission.<sup>[59]</sup> Copyright 2018, Wiley.



## Author Photographs

*Dr. Lorène Tallet received her M.S (2016) in microbiology from the university of Strasbourg (France). She performed a PhD thesis in the field of smart antimicrobial surfaces at the University of Strasbourg, France. During this period, she worked on multilayer films made of poly(arginine) and hyaluronic acid whose antibacterial activity is induced by the presence of pathogen. Now, she is employed as a postdoctoral fellow and still works on smart biomaterials and antiviral coatings.*



*Dr. Philippe Lavallo holds a PhD degree in Biophysics in 1998 from University of Strasbourg. Then he moved to the Biozentrum in Basel (Switzerland) to study the mechanism of the antifreeze glycoproteins. He got the position of "Research Director" at Inserm in 2011. Since 2013, he co-manages as deputy director the Inserm Unit "Biomaterials and Bioengineering" in Strasbourg, France. He focuses his research on the design of new materials/coatings with innovative properties for biomedical applications.*



**Table of contents entry**

Medical device-associated infections, together with resistance to antibiotics, are growing problems worldwide. To reduce the development of resistance, new antibacterial systems that locally respond to bacterial infections are being increasingly studied. In this progress report, the most cutting-edge approaches of smart antibacterial drug delivery systems are described.

**Keyword**

Smart surfaces, hydrogels, nanomaterial, coatings, antimicrobial

ToC Figure

